arXiv:1412.0956v1 [cond-mat.stat-mech] 2 Dec 2014

Microscopic theory for negative differential mobility in crowded environments

O. Bénichou, P. Illien, G. Oshanin, A. Sarracino, and R. Voituriez
Sorbonne Universités, UPMC Univ Paris 06, UMR 7600, LPTMC, F-75005, Paris, France and
CNRS, UMR 7600, Laboratoire de Physique Théorique de la Matière Condensée, F-75005, Paris, France

We study the behavior of the stationary velocity of a driven particle in an environment of mobile hard-core obstacles. Based on a lattice gas model, we demonstrate analytically that the drift velocity can exhibit a nonmonotonic dependence on the applied force, and show quantitatively that such negative differential mobility (NDM), observed in various physical contexts, is controlled by both the density and diffusion time scale of obstacles. Our study unifies recent numerical and analytical results obtained in specific regimes, and makes it possible to determine analytically the region of the full parameter space where NDM occurs. These results suggest that NDM could be a generic feature of biased (or active) transport in crowded environments.

PACS numbers: 83.10.-y,05.40.Fb,83.10.Pp

Introduction.–Quantifying the response of a complex system to an external force is one of the cornerstone problems of statistical mechanics. In the linear response regime, a fundamental result is the fluctuation-dissipation theorem, which relates system response and spontaneous fluctuations. Within the last years a great effort has been devoted to generalizations of this theorem to nonequilibrium situations [1–4], when the time reversal symmetry is broken, and also to elucidating the effects of the higher order contributions in the external perturbation [5–11]. From experimental perspective, theoretical understanding of the latter issues is of an utmost importance in several fields, such as active microrheology [12–14] and dynamics of nonequilibrium fluids [15, 16].

A striking example of anomalous behavior beyond the linear regime is the negative response of a particle's velocity to an applied force, observed in diverse situations in which a particle subject to an external force F travels through a medium. The terminal drift velocity $V(F)$ attained by the driven particle is then a nonmonotonic function of the force: upon a gradual increase of F, the terminal drift velocity first grows as expected from linear response, reaches a peak value and eventually decreases. This means that the differential mobility of the driven particle becomes negative for F exceeding a certain threshold value. Such a counter-intuitive "getting more from pushing less" [17] behavior of the differential mobility (or of the differential conductivity) has been observed for a variety of physical systems and processes, e.g. for electron transfer in semiconductors at low temperatures [18–21], hopping processes in disordered media [22], transport of electrons in mixtures of atomic gases with reactive collisions [23], far-from-equilibrium quantum spin chains [24], some models of Brownian motors [25, 26], soft matter colloidal particles [27], different nonequilibrium systems [17], and also for the kinetically constrained models of glass formers [28–30].

Apart of these examples, negative differential mobility (NDM) has been observed in the minimal model of a driven lattice gas, which captures many essential features of the behavior in realistic systems. In this model one focuses on the dynamics of a hard-core tracer particle (TP) which performs a random walk of mean waiting time τ, biased by an external force F, on a lattice containing a bath of hard-core particles (or "obstacles") of density ρ, which perform symmetric random walks of mean waiting time τ^*. Such a system may be viewed as the combination of two paradigmatic models of nonequilibrium statistical mechanics, namely the symmetric and asymmetric exclusion processes, which have been extensively studied to describe heat and particles transport properties [31]. Up to now, only limiting situations of this model have been analyzed.

In the case of *immobile* bath particles ($\tau^* \to \infty$), it has been argued that for a tracer subject to an external force and diffusing on an infinite percolation cluster, the drift velocity vanishes for large enough values of the force, and therefore NDM occurs [32]. More recently, NDM was also observed via numerical simulations for low density of immobile particles [2, 34] and analytically accounted for [2], but to the first order in ρ only. Surprisingly enough, it appears that NDM is not a specific feature of a frozen distribution of obstacles but also emerges in dynamical environments undergoing continuous reshuffling due to obstacles random motion ($\tau^* < \infty$). Indeed, very recently, numerical analysis performed in [35] at a specific value of the density revealed that NDM could occur in a 2D driven lattice gas for bath particles diffusing slow enough.

In general, the origin of the NDM has been attributed to the nonequilibrium (called "frenetic") contributions appearing in the fluctuation-dissipation relation [36, 37]. As shown earlier in [38, 39], due to its interactions with the environment the TP drives such a crowded system to a nonequilibrium steady-state with a nonhomogeneous obstacles density profile. However, the "nonequilibrium" condition is clearly not the only necessary condition for the NDM to emerge - in simulations in [35] this phenomenon is apparent for some range of parameters but it definitely should be absent when the obstacles move sufficiently fast so that the TP sees the environment as a fluid.

Finally, NDM seems to be controlled by both the density ρ and the diffusion time scale τ^* of the bath particles.

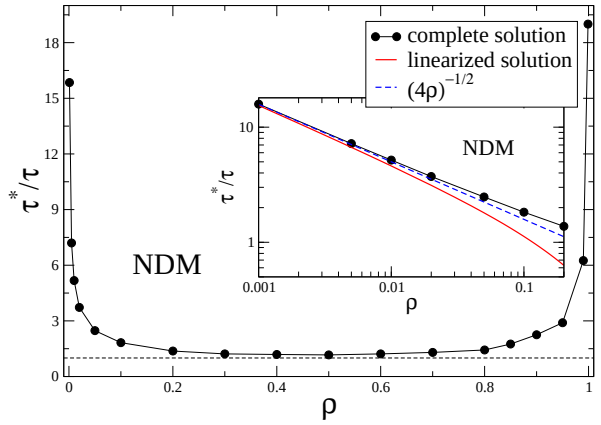

FIG. 1. (Color online) Region of negative differential mobility (NDM) in the plane τ^*/τ vs ρ, for $d = 2$ (black circles), as revealed by our analytical approach. Inset: zoom of the low density region and comparison with the prediction of the linear approximation, Eq. (33) (red line), and with asymptotic result, Eq. (5) (blue dashed line).

However, a microscopic theoretical analysis of this effect is still lacking. The only available analysis is restricted to the case of immobile obstacles (in the low density regime) where, by definition, the bath particles are not perturbed by the TP. In this Letter, we reveal the complete scenario of this coupled dynamics providing i) a scaling argument in the dilute regime that unveils the physical mechanism of NDM, ii) an analytic analysis of the TP velocity for arbitrary values of system parameters, and iii) a criterion for the NDM effect to be observed, which shows in particular that for any ρ NDM exists if τ^* is large enough (see Fig. 1).

More precisely, using a decoupling of relevant correlation functions, we derive the force-velocity relation $V(F)$ valid for general ρ, τ, τ^* and F, and for any dimension $d \geq 2$. This approximate expression is shown to be exact both in the dilute and in the dense limit and provides results in excellent agreement with numerical simulations for a wide range of parameters. In the low density regime, we recover the exact result obtained in [2] in the limit $\rho \to 0$ and $\tau^* \to \infty$, while in the high density limit our general expression gives back the exact results of [40]. Therefore, our theoretical framework unifies existing asymptotic results [2, 34, 35]. Our analytic result also allows us to quantify the non-trivial nonmonotonic behavior of the velocity with respect to the force, bringing to the fore the central role of the coupling between density and time scales. In particular, we analytically determine in the plane $(\rho, \tau^*/\tau)$ the region for NDM and establish an accurate criterion for the existence of the NDM (exact at linear order in ρ), see Fig. 1 [41].

Model.–The dynamics in the system under study is defined as follows. Each bath particle, selected at random, waits an exponential time with mean τ^* and then selects the jump direction with probability $1/2d$. Once the jump direction is chosen, the obstacle attempts to move onto the target site: the move is realized if the target site is empty at this time moment; otherwise, if the target site is occupied by either another obstacle or the TP - the move is rejected. In a similar fashion, the TP waits an exponential time with mean τ and then chooses to jump in the direction ν ($\nu \in \{\pm 1, \ldots, \pm d\}$) with probability

$$p_\nu = \frac{e^{(\beta/2)\boldsymbol{F}\cdot\boldsymbol{e}_\nu}}{\sum_\mu e^{(\beta/2)\boldsymbol{F}\cdot\boldsymbol{e}_\mu}}, \tag{1}$$

where β is the inverse temperature (measured in the units of the Boltzmann constant), $\boldsymbol{e}_\mu$ are the corresponding $2d$ base vectors of the hypercubic lattice, the lattice step has been taken equal to one and we denote $\boldsymbol{F} \equiv F\boldsymbol{e}_1$. Note that (1) provides the standard choice of the transition probabilities, which satisfy the generalized detailed balance condition [42], but arbitrary choices of p_ν [35] can be considered within our formalism [43].

Before discussing the mathematical details of our approach, we first present a scaling argument that reveals the physical mechanism underlying NDM and provides an estimation of the threshold in the low density limit. Assuming a strong external force, one has $p_1 \simeq 1 - \epsilon$, $p_{-1} = \mathcal{O}(\epsilon^2)$ with $\epsilon = 2\exp(-\beta F/2)$, so that the mean velocity in the absence of obstacles can be written $(1-\epsilon)/\tau$. The stationary velocity in the presence of obstacles is then given by the mean distance $1/\rho$ travelled by the TP between two obstacles divided by the mean duration of this excursion, which is the sum of the mean time of free motion $\tau/[\rho(1-\epsilon)]$ and of the mean trapping time $\tau_{\rm trap}$ per obstacle. The escape from a trap results from two alternative independent events: the TP steps in the transverse direction (with rate ϵ/τ) or the obstacle steps away (with rate $3/(4\tau^*)$, for $d = 2$). This leads to $1/\tau_{\rm trap} = 3/(4\tau^*) + \epsilon/\tau$, and finally

$$V(F) = \frac{1-\epsilon}{\tau + 4\rho(1-\epsilon)\frac{\tau^*}{3+4\epsilon\tau^*/\tau}}. \tag{2}$$

From this formula, it can be viewed that V is decreasing with F at large F (i.e. small ϵ), and therefore non monotonic with F, as soon as $\tau^* \gtrsim \tau/\sqrt{\rho}$. This unveils the physical origin of NDM in the dilute regime, where two effects compete. On the one hand a large force reduces the travel time between two consecutive encounters with bath particles; on the other hand it increases the escape time from traps created by surrounding particles. Eventually, for τ^* large enough, such traps are sufficiently long lived to slow down the TP when F is increased. In order to get a rigorous and quantitative understanding of NDM for all parameter values, we now analyze in detail the microscopic dynamics of the model.

General expression of the velocity.– Let the Boolean variable $\eta(\boldsymbol{R}) = \{1, 0\}$ denote the instantaneous occupation of the site at position $\boldsymbol{R}$ by any of the obstacles, $\eta \equiv \{\eta(\boldsymbol{R})\}$ denote the instantaneous configuration of all such occupation variables and $\boldsymbol{R}_{TP}$ - the instantaneous position of the driven particle. The stationary velocity

$V(F)$ along the field direction is easily shown to be given by (see Supplementary Material [44])

$$V(F) \equiv \frac{d\langle \boldsymbol{R}_{TP} \cdot \boldsymbol{e}_1 \rangle}{dt} = \frac{1}{2d\tau^*}(A_1 - A_{-1}), \qquad (3)$$

where the coefficients A_ν ($\nu = \pm 1, \ldots, \pm d$) are defined by the relation $A_\nu \equiv 1 + \frac{2d\tau^*}{\tau} p_\nu (1 - k(\boldsymbol{e}_\nu))$. Here, $k(\boldsymbol{e}_\nu) \equiv \sum_{\boldsymbol{R}_{TP},\eta} \eta(\boldsymbol{R}_{TP}+\boldsymbol{e}_\nu) P(\boldsymbol{R}_{TP}, \eta)$ represents the stationary density profile around the TP, $P(\boldsymbol{R}_{TP}, \eta)$ being the joint probability of finding the TP at the site $\boldsymbol{R}_{TP}$ with the configuration of obstacles η.

In order to obtain a general expression for the TP stationary velocity for arbitrary force, we make use of the decoupling approximation [46] for the correlation function of the occupation variables of the form

$$\langle \eta(\boldsymbol{R}_{TP}+\boldsymbol{\lambda}) \eta(\boldsymbol{R}_{TP}+\boldsymbol{e}_\nu) \rangle \approx \langle \eta(\boldsymbol{R}_{TP}+\boldsymbol{\lambda}) \rangle \langle \eta(\boldsymbol{R}_{TP}+\boldsymbol{e}_\nu) \rangle, \qquad (4)$$

which presumes that the occupation of the site just in front of the TP, and of a site some distance λ apart of it, become statistically independent. This approach represents a mean-field-like approximation and its physical motivation relies on the observation that a fluctuation in the occupancy of the sites in the vicinity of the tracer does not affect the dynamics far from the tracer itself. This decoupling scheme has been previously used in [38, 39] to derive general equations for the TP velocity in two-dimensional open systems. However, the analysis in [38, 39] has only been concerned with the linear response regime, giving access to the Stokesian behavior of the mobility and hence, via the Einstein relation, to the diffusion coefficient of the particle in the absence of external bias. Here we extend this analysis to nonlinear response (arbitrary force) and arbitrary dimensionality of the embedding lattice in order to define the physical conditions under which the NDM takes place.

Following [39], this decoupling approximation can be shown to lead to a closed system for the A_ν, which is reported in [44]. This system is highly nonlinear in the coefficients A_ν. However, it can be numerically solved to find the analytic value of the TP velocity for an arbitrary choice of the model parameters.

Criterion for NDM.–By using our analytical solution, the region for NDM in the plane $(\rho, \tau^*/\tau)$ can be determined, as reported in Fig. 1, which constitutes the key result of this Letter. Importantly, this shows that for every density there exists a value of τ^*/τ above which NDM can be observed; this value diverges for both $\rho \to 0$ and $\rho \to 1$. In turn, for any value of $\tau^*/\tau \gtrsim 1$, there exists a range of density $[\rho_1, \rho_2]$, for which NDM occurs. When τ^*/τ is sufficiently large, the value of ρ_1 can be made explicit using a small density expansion (see Eqs.(6)-(33) below). This leads to the exact asymptotic result

$$\rho_1 \underset{\tau^*/\tau \to \infty}{\sim} \frac{1}{4} \left(\frac{\tau}{\tau^*} \right)^2, \qquad (5)$$

which is validated numerically in Fig. 1, see [44]. Note that this exact result is consistent with our earlier scaling argument.

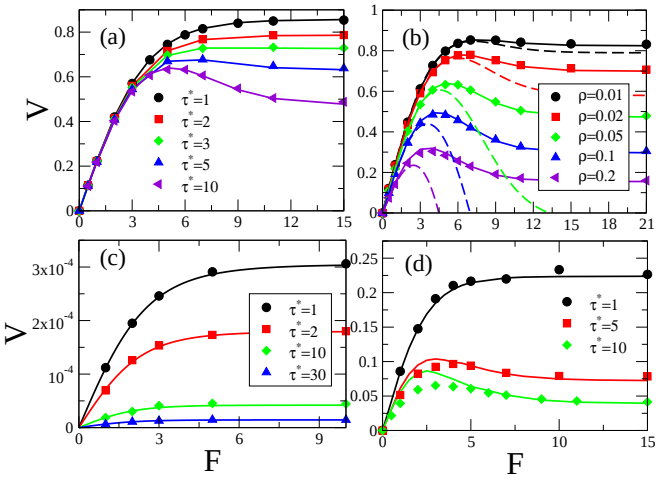

FIG. 2. (Color online). $V(F)$ for $d = 2$ and $\beta = 1$: (a) $\rho = 0.05$, $\tau = 1$ and different τ^*, analytic prediction (lines) and numerical simulations (symbols); (b) $\tau = 1$ and $\tau^* = 10$, analytic prediction (continuous lines), numerical simulations (symbols) and linearized solution (dashed lines); (c) high density limit, $\rho = 0.999$, with $\tau = 1$ and different τ^*, analytic prediction of Eq. (9) (lines) and numerical simulations (symbols); (d) $\rho = 0.5$, $\tau = 1$ and different τ^*, analytic prediction (lines) and numerical simulations (symbols).

In order to validate the above scenario and to explore the effectiveness of the decoupling approximation (14), we have performed numerical simulations for different dimensions. A very good agreement is observed for a wide range of parameters (see Fig. 2 for a two-dimensional infinite square lattice and [44] for the three-dimensional case). We show below that this approximation is actually exact in both limits $\rho \to 0$ (at linear order in ρ) and $\rho \to 1$.

Low density limit. – In the dilute limit $\rho \to 0$, the system for the coefficients A_μ can be drastically simplified (see [44]). In this case, one has $A_\mu \sim 1 + (2d\tau^*/\tau)p_\mu$ and the TP velocity can be expressed as

$$V(\rho \to 0) = \frac{1}{\tau}(p_1 - p_{-1}) - \frac{\rho}{\tau}(p_1 - p_{-1} + p_1 v_1 - p_{-1} v_{-1}) + o(\rho), \qquad (6)$$

where the coefficients $v_{\boldsymbol{n}}$ satisfy the linear system of equations

$$2d(1 + \tau^*/\tau) v_{\boldsymbol{n}} = \sum_\nu [1 + (2d\tau^*/\tau) p_\nu] v_{\boldsymbol{e}_\nu} \nabla_{-\nu} \mathcal{F}_{\boldsymbol{n}} - (2d\tau^*/\tau)(p_1 - p_{-1})(\nabla_1 - \nabla_{-1}) \mathcal{F}_{\boldsymbol{n}}. \qquad (7)$$

Here, the functions $\mathcal{F}_{\boldsymbol{n}}$ depend on the coefficients A_μ, on dimension of the system, and are reported explicitly in [44], while ∇_μ is a differential operator defined by the relation $\nabla_\mu f(\boldsymbol{\lambda}) \equiv f(\boldsymbol{\lambda}+\boldsymbol{e}_\mu) - f(\boldsymbol{\lambda})$. The $V(F)$ obtained in this dilute limit is reported in Fig. 2(b) (dashed lines) for different densities and shows the same behavior as the

complete solution, even at intermediate values of ρ, for small enough forces.

A further simplification occurs in the limit considered in [2] of the standard Lorentz gas, namely when $\tau^*/\tau \to \infty$. In this case, from (33) we obtain an explicit solution, which, as an actual fact, coincides with the analytic results presented in [2]. In the particular case $d = 2$, the functions $\mathcal{F}_{\boldsymbol{n}}$ simplify to

$$\mathcal{F}_{\boldsymbol{n}} = e^{-n_1 F/2} \int_0^\infty e^{-t} \mathrm{I}_{n_1}(2t/Z)\mathrm{I}_{n_2}(2t/Z)dt, \quad (8)$$

with $Z = 2 + e^{\beta F/2} + e^{-\beta F/2}$. Substituting Eq. (34) into the system (33), and using Eq. (6), one recovers the exact result of [2] (see [44]). As the accuracy of our analytic results increases when τ^*/τ decreases, as shown numerically in Fig. 2, we claim that our decoupling approximation, Eq. (14), is exact at linear order in ρ.

High density limit.–As detailed in [44] and illustrated here in the particular case $d = 2$, the system for the coefficients A_μ linearized around $1 - \rho$ leads to

$$V(F) = \frac{1}{\tau}(1-\rho)\frac{\sinh(\beta F/2)}{1 + \cosh(\beta F/2)[1 + \frac{2\tau^*}{\tau}(\pi - 2)]}. \quad (9)$$

This result gives back the exact expression obtained in [40] in the particular case $\tau = \tau^*$.

Conclusion.–We have presented an analytic theory for NDM in a general driven lattice gas. Exploiting a decoupling approximation, we have obtained an analytic expression for the force velocity relation. This expression which goes beyond linear response, is shown to be exact in both $\rho \to 0$ and $\rho \to 1$ regimes and turns out to be in very good agreement with numerical simulations for a wide range of parameters. In particular, for values of τ^* large enough, a nonmonotonic behavior of the TP velocity as a function of the external force is indeed observed. Our study extends analytical results obtained in [2] and sheds light on recent numerical observations [34, 35]. In particular, with the choice of transition rates of [35], which do not depend on the field in the transverse direction, NDM is observed only for much larger values of τ^*/τ. This is due to the fact that the escape time of the TP from traps, in that case, is insensitive to the applied force to linear order in ρ.

Our solution reveals and quantifies a minimal physical mechanism responsible for NDM, which is based on the coupling between the density of obstacles and the diffusion time scales of the TP and obstacles. Our minimal model, which takes into account the repulsive part of the particle-particle interactions only, suggests that the phenomenon of the negative differential mobility should be a generic feature of biased transport in crowded environments.

The work of O.B. and A.S. is supported by the European Research Council (Grant No. FPTOpt-277998).

[1] U. Marini Bettolo Marconi, A. Puglisi, L. Rondoni, and A. Vulpiani, Phys. Rep. **461**, 111 (2008).
[2] L. Cugliandolo, J. Phys. A **44**, 483001 (2011).
[3] U. Seifert, Rep. Prog. Phys. **75**, 126001 (2012).
[4] G. Gradenigo, A. Puglisi, A. Sarracino, D. Villamaina, and A. Vulpiani, in *Nonequilibrium Statistical Physics of Small Systems: Fluctuation Relations and Beyond*, Eds.: R. Klages, W. Just and C. Jarzynski, (Wiley-VCH, Weinheim, 2012)
[5] A. Morita, Phys. Rev. A **34**, 1499 (1986).
[6] J.-P. Bouchaud and G. Biroli, Phys. Rev. B **72**, 064204 (2005).
[7] E. Lippiello, F. Corberi, A. Sarracino, and M. Zannetti, Phys. Rev. B **77**, 212201 (2008); Phys. Rev. E **78**, 041120 (2008).
[8] G. Diezemann, Phys. Rev. E **85**, 051502 (2012).
[9] O. Bénichou, P. Illien, G. Oshanin, and R. Voituriez, Phys. Rev. E **87**, 032164 (2013).
[10] P. Illien, O. Bénichou, C. Mejia-Monasterio, G. Oshanin, and R. Voituriez, Phys. Rev. Lett. **111**, 038102 (2013)
[11] O. Bénichou, A. Bodrova, D. Chakraborty, P. Illien, A. Law, C. Mejia-Monasterio, G. Oshanin, and R. Voituriez, Phys. Rev. Lett. **111**, 260601 (2013)
[12] P. Habdas, D. Schaar, A. C. Levitt, and E. R. Weeks, Europhys. Lett. **67**, 477 (2004).
[13] T. M. Squires, and T. G. Mason, Ann. Rev. Fluid Mech. **42**, 413 (2009).
[14] L. G. Wilson, A. W. Harrison, A. B. Schofield, J. Arlt, and W. C. K. Poon, J. Phys. Chem. B **113**, 3806 (2009).
[15] D. J. Evans, and G. Morriss. *Statistical Mechanics of Non-equilibrium Liquids*, (Cambridge University Press, 2008).
[16] N. J. Wagner, and J. F. Brady, Physics Today **62**, 27 (2009).
[17] R. K. P. Zia, E. L. Praestgaard, and O. G. Mouritsen, Am. J. Phys. **70**, 384 (2002).
[18] E. Conwell, Physics Today **23**, 35 (1970).
[19] F. Nava, C. Canali, F. Catellani, G. Gavioli, and G. Ottaviani, J. Phys. C: Solid State Phys. **9**, 1685 (1976).
[20] C. J. Stanton, H. U. Baranger, and J. W. Wilkins, Appl. Phys. Lett. **49**, 176 (1986).
[21] X. L. Lei, N. J. M. Horing, and H. L. Cui, Phys. Rev. Lett. **66**, 3277 (1991).
[22] H. Böttger and V. V. Bryksin, Phys. Stat. Sol. (B) **113**, 9 (1982).
[23] see, e.g., S. B. Vrhovac and Z. Lj. Petrovic, Phys. Rev. E **53**, 4012 (1996).
[24] G. Benenti, G. Casati, T. Prosen, and D. Rossini, Europhys. Lett. **85**, 37001 (2009).
[25] G. W. Slater, H. L. Guo, and G. I. Nixon, Phys. Rev. Lett. **78**, 1170 (1997).
[26] M. Kostura, L. Machura, P. Hänggi, J. Luczka, and P. Talkner, Physica A **371**, 20 (2006).
[27] R. Eichhorn, J. Regtmeier, D. Anselmetti, and P. Reimann, Soft Matter **6**, 1858 (2010).
[28] R. L. Jack, D. Kelsey, J. P. Garrahan, and D. Chandler,

Phys. Rev. E **78**, 011506 (2008).
[29] M. Sellitto, Phys. Rev. Lett. **101**, 048301 (2008).
[30] F. Turci, E. Pitard, and M. Sellitto, Phys. Rev. E **86**, 031112 (2012).
[31] T. Chou, K. Mallick, R. K. P. Zia, Rep. Prog. Phys. **74**, 116601 (2011).
[32] M. Barma and D. Dhar, J. Phys.: Solid State Phys. **16**, 1451 (1983).
[33] S. Leitmann and T. Franosch, Phys. Rev. Lett. **111**, 190603 (2013).
[34] P. Baerts, U. Basu, C. Maes, and S. Safaverdi, Phys. Rev. E **88**, 052109 (2013).
[35] U. Basu and C. Maes, J. Phys. A: Math. Theor. **47**, 255003 (2014).
[36] E. Lippiello, F. Corberi, and M. Zannetti, Phys. Rev. E **71**, 036104 (2005).
[37] M. Baiesi, C. Maes, and B. Wynants, Phys. Rev. Lett. **103**, 010602 (2009).
[38] O. Bénichou, A. M. Cazabat, J. De Coninck, M. Moreau, and G.Oshanin, Phys. Rev. Lett. **84**, 511 (2000).
[39] O. Bénichou, A. M. Cazabat, J. De Coninck, M. Moreau, and G. Oshanin, Phys. Rev. B **63**, 235413 (2001).
[40] O. Bénichou, and G. Oshanin, Phys. Rev. E **66**, 031101 (2002).
[41] Let us notice that the change of behavior observed in the model does not represent a genuine phase transition occurring in the system.
[42] J. L. Lebowitz and H. Spohn, J. Stat. Phys **95**, 333 (1999).
[43] The choice of transition rates studied in [35] corresponds to take, for $d = 2$, $p_1 = (1/2)e^{\beta F/2}/(e^{\beta F/2} + e^{-\beta F/2}), p_{-1} = (1/2)e^{-\beta F/2}/(e^{\beta F/2} + e^{-\beta F/2})$ and $p_2 = p_{-2} = 1/4$, with $\tau = 1/2$ and $\tau^* = 1/4\gamma$, where γ is the inverse time-scale introduced in [35].
[44] See Supplemental Material [url], which includes Ref. [45], for details on the calculations and numerical simulations.
[45] B. D. Hughes, *Random Walks and Random Environments* (Oxford Science, Oxford, 1995).
[46] S. F. Burlatsky, G. Oshanin, M. Moreau, and W. P. Reinhardt, Phys. Rev. E **54**, 3165 (1996).

Supplemental Material

I. COMPUTATION OF THE STATIONARY VELOCITY

The time evolution of the joint probability $P(\boldsymbol{R}_{TP},\eta;t)$ of finding at time t the TP at the site with the configuration of obstacles η, is governed by the following master equation

$$\partial_t P(\boldsymbol{R}_{TP},\eta;t) = \frac{1}{2d\tau^*}\sum_{\mu=1}^{d}\sum_{\boldsymbol{r}\neq\boldsymbol{R}_{TP}-\boldsymbol{e}_\mu,\boldsymbol{R}_{TP}} [P(\boldsymbol{R}_{TP},\eta^{\boldsymbol{r},\mu};t)-P(\boldsymbol{R}_{TP},\eta;t)]$$

$$+\frac{1}{\tau}\sum_{\mu=1}^{d} p_\mu\{[1-\eta(\boldsymbol{R}_{TP})]P(\boldsymbol{R}_{TP}-\boldsymbol{e}_\mu,\eta;t)-[1-\eta(\boldsymbol{R}_{TP}+\boldsymbol{e}_\mu)]P(\boldsymbol{R}_{TP},\eta;t)\}, \tag{10}$$

where $\eta^{\boldsymbol{r},\mu}$ is the configuration obtained from η by exchanging the occupation numbers of sites $\boldsymbol{r}$ and $\boldsymbol{r}+\boldsymbol{e}_\mu$.

The stationary velocity of the TP is obtained by multiplying both sides of the master equation by $(\boldsymbol{R}_{TP}\cdot\boldsymbol{e}_1)$, summing over all possible configurations $(\boldsymbol{R}_{TP},\eta)$, and taking the limit $t\to\infty$. This yields the expression

$$V = \frac{1}{\tau}\left\{p_1\left[1-k(\boldsymbol{e}_1)\right]-p_{-1}\left[1-k(\boldsymbol{e}_{-1})\right]\right\}, \tag{11}$$

where the functions $k(\boldsymbol{\lambda})$ are the stationary values (in the $t\to\infty$ limit) of $k(\boldsymbol{\lambda};t)$, defined as

$$k(\boldsymbol{\lambda};t) = \sum_{\boldsymbol{R}_{TP},\eta}\eta(\boldsymbol{R}_{TP}+\boldsymbol{\lambda})P(\boldsymbol{R}_{TP},\eta;t). \tag{12}$$

We define $k(\boldsymbol{\lambda};t)$ for $\boldsymbol{\lambda}=\boldsymbol{0}$ by $k(\boldsymbol{0};t)=0$. The evolution equations for $k(\boldsymbol{\lambda};t)$ may be obtained by multiplying the master equation by $\eta(\boldsymbol{R}_{TP}+\boldsymbol{\lambda})$ and summing over all the configurations of $(\boldsymbol{R}_{TP},\eta)$. We get the following equation:

$$2d\tau^*\partial_t k(\boldsymbol{\lambda};t) = \sum_\mu\left(\nabla_\mu-\delta_{\boldsymbol{\lambda},\mathbf{e_\mu}}\nabla_{-\mu}\right)k(\boldsymbol{\lambda};t)+\frac{2d\tau^*}{\tau}\sum_\nu p_\nu\left\langle[1-\eta(\boldsymbol{R}_{TP}+\mathbf{e_\nu})]\nabla_\nu\eta(\boldsymbol{R}_{TP}+\boldsymbol{\lambda})\right\rangle, \tag{13}$$

where we introduced the average $\langle X(\boldsymbol{R})\rangle \equiv \sum_{\boldsymbol{R}_{TP},\eta}X(\boldsymbol{R})P(\boldsymbol{R}_{TP},\eta;t)$, and ∇_μ is a differential operator defined by the relation $\nabla_\mu f(\boldsymbol{\lambda}) \equiv f(\boldsymbol{\lambda}+\boldsymbol{e}_\mu)-f(\boldsymbol{\lambda})$. In order to solve this equation, we use the decoupling approximation proposed in the main text:

$$\langle\eta(\boldsymbol{R}_{TP}+\boldsymbol{\lambda})\eta(\boldsymbol{R}_{TP}+\boldsymbol{e}_\nu)\rangle \approx \langle\eta(\boldsymbol{R}_{TP}+\boldsymbol{\lambda})\rangle\langle\eta(\boldsymbol{R}_{TP}+\boldsymbol{e}_\nu)\rangle, \tag{14}$$

which is valid for $\boldsymbol{\lambda}\neq\boldsymbol{e}_\nu$. For convenience, we also introduce the functions $h(\boldsymbol{\lambda};t)$, defined by

$$h(\boldsymbol{\lambda};t) \equiv k(\boldsymbol{\lambda};t)-\rho. \tag{15}$$

One finally shows that $h(\boldsymbol{\lambda};t)$ satisfy the following evolution equations

$$2d\tau^*\partial_t h(\boldsymbol{\lambda};t) = \widetilde{L}h(\boldsymbol{\lambda};t) \quad \text{for} \quad \boldsymbol{\lambda}\notin\{\boldsymbol{0},\pm\boldsymbol{e}_1,\ldots,\pm\boldsymbol{e}_d\} \tag{16}$$

$$2d\tau^*\partial_t h(\boldsymbol{\lambda};t) = \widetilde{L}h(\boldsymbol{\lambda};t)+\rho(A_\nu-A_{-\nu}) \quad \text{for} \quad \boldsymbol{\lambda}\in\{\boldsymbol{0},\pm\boldsymbol{e}_1,\ldots,\pm\boldsymbol{e}_d\}, \tag{17}$$

with $\widetilde{L}\equiv\sum_\mu A_\mu\nabla_\mu$ and $A_\mu = 1+(2d\tau^*/\tau)p_\mu[\rho_0-h(\boldsymbol{e}_\mu)]$.

We introduce the auxiliary variable $\boldsymbol{\xi}=(\xi_1,\ldots,\xi_d)$ and the generating function

$$H(\boldsymbol{\xi};t) = \sum_{n_1=-\infty}^{\infty}\sum_{n_2,\cdots,n_d=0}^{L-1} h_{n_1,\cdots,n_d}(t)\prod_{j=2}^{d}\xi_j^{n_j}, \tag{18}$$

where the shorthand notation $h(n_1\boldsymbol{e}_1+\cdots+n_d\boldsymbol{e}_d;t) = h_{n_1,\ldots,n_d}(t)$ has been used. $(n_1,\ldots,n_d)$ are the components of the vector $\boldsymbol{n}$. If $(n_1,\ldots,n_d)=\boldsymbol{e}_\nu$ then we use $h_{\boldsymbol{e}_\nu}\equiv h_\nu$. From Eqs. (16) and (17) we can show that $H(\boldsymbol{\xi};t)$ is the solution of the following partial differential equation

$$2d\tau^*\partial_t H(\boldsymbol{\xi};t) = \left[\frac{A_1}{\xi_1}+A_{-1}\xi_1+A_2\sum_{j=2}^{d}\left(\frac{1}{\xi_j}+\xi_j\right)-\alpha\right]H(\boldsymbol{\xi};t)+K(\boldsymbol{\xi};t), \tag{19}$$

with $\alpha = A_1 + A_{-1} + 2(d-1)A_2$ and

$$K(\boldsymbol{\xi};t) \equiv A_1(\xi_1 - 1)h_1(t) + A_{-1}\left(\frac{1}{\xi_1} - 1\right)h_{-1}(t) + A_2\sum_{j=2}^{d}\left[(\xi_j - 1)h_j(t) + \left(\frac{1}{\xi_j} - 1\right)h_{-j}(t)\right] + \rho(A_1 - A_{-1})\left(\xi_1 - \frac{1}{\xi_1}\right). \tag{20}$$

The stationary solution of Eq. (19) is

$$H(\boldsymbol{\xi}) = \frac{K(\boldsymbol{\xi})}{\alpha}\frac{1}{1 - \left[\frac{A_1}{\alpha}\frac{1}{\xi_1} + \frac{A_{-1}}{\alpha}\xi_1 + \frac{A_2}{\alpha}\sum_{j=2}^{d}\left(\frac{1}{\xi_j} + \xi_j\right)\right]}. \tag{21}$$

We rewrite the auxiliary variables as $\xi_j = \mathrm{e}^{iq_j}$, and introduce the function

$$\mathcal{F}_{\boldsymbol{n}} = \frac{1}{(2\pi)^d}\int_{[-\pi,\pi]^d} dq_1 \dots dq_d \frac{\prod_{j=1}^{d}\mathrm{e}^{-in_j q_j}}{1 - \lambda(q_1,\dots,q_d)} \tag{22}$$

with

$$\lambda(q_1,\dots,q_d) = \frac{A_1}{\alpha}\mathrm{e}^{-iq_1} + \frac{A_{-1}}{\alpha}\mathrm{e}^{iq_1} + \frac{2A_2}{\alpha}\sum_{j=2}^{d}\cos q_j, \tag{23}$$

so that $H(\boldsymbol{\xi})$ becomes

$$H(q_1,\dots,q_d) = \frac{K(q_1,\dots,q_d)}{\alpha}\frac{1}{1 - \lambda(q_1,\dots,q_d)}. \tag{24}$$

Note that $\mathcal{F}_{\boldsymbol{n}}$ is the long-time limit of the generating function of a biased random walk on d-dimensional lattice [1]. Using the definition of $\mathcal{F}_{\boldsymbol{n}}$ from Eq. (22), and taking the inverse Fourier transforms, we get

$$\frac{1}{1 - \lambda(q_1,\dots,q_d)} = \sum_{n_1,\dots,n_d=-\infty}^{\infty}\left(\prod_{j=1}^{d} e^{i\pi n_j q_j}\right)\mathcal{F}_{n_1,\dots,n_d}. \tag{25}$$

Using Eq. (24),

$$H(q_1,\dots,q_d) = \frac{1}{\alpha}\sum_{n_1,\dots,n_d=-\infty}^{\infty} K(q_1,\dots,q_d)\mathcal{F}_{n_1,\dots,n_d}\prod_{j=1}^{d} e^{in_j q_j}. \tag{26}$$

Finally, using the definition of K in Eq. (20), writing $H(q_1,\dots,q_d)$ using Eq. (18) and identifying the terms from both sides of Eq. (26), one shows that $h_{n_1,\dots,n_d}$ is given by the following system of $2d$ equations

$$\alpha h_{n_1,\dots,n_d} = \sum_{\nu} A_\nu h_\nu \nabla_{-\nu}\mathcal{F}_{n_1,\dots,n_d} - (1-\rho_0)(A_1 - A_{-1})(\nabla_1 - \nabla_{-1})\mathcal{F}_{n_1,\dots,n_d}, \tag{27}$$

where $(n_1,\dots,n_d)$ are taken equal to the coordinates of the base vectors $\{\pm\boldsymbol{e}_1,\dots,\pm\boldsymbol{e}_d\}$. Noticing that $h_{\pm 2} = \dots = h_{\pm d}$ for symmetry reasons, this system of $2d$ equations may be reduced to a system of three equations ($\nu = \pm 1, 2$)

$$A_\nu = 1 + \frac{2d\tau^*}{\tau}p_\nu\left[1 - \rho - \rho(A_1 - A_{-1})\frac{\det C_\nu}{\det C}\right]. \tag{28}$$

In the above expressions the matrix $C \equiv (A_\mu\nabla_{-\mu}\mathcal{F}_{\boldsymbol{e}_\nu} - \alpha\delta_{\mu,\nu})_{\mu,\nu}$, $\alpha = \sum_\mu A_\mu$, and the matrix C_ν is obtained from the matrix C by replacing the column corresponding to the index ν with the column vector $((\nabla_1 - \nabla_{-1})\mathcal{F}_{\boldsymbol{e}_\nu})_\nu$.

Notice that the functions $\mathcal{F}_{\boldsymbol{n}}$, defined in (22) can be rewritten as

$$\mathcal{F}_{\boldsymbol{n}} = \left(\frac{A_{-1}}{A_1}\right)^{n_1/2}\int_0^\infty e^{-t}\mathrm{I}_{n_1}(2\alpha^{-1}\sqrt{A_1 A_{-1}}t)\prod_{i=2}^{d}\mathrm{I}_{n_i}(2\alpha^{-1}A_2 t)dt, \tag{29}$$

n_i being the components of the base vector $\boldsymbol{n}$ and $\mathrm{I}_i(x)$ - the modified Bessel function of first kind.

II. LINEARIZED SOLUTION FOR LOW DENSITY

For the general $d-$dimensional case the functions $h_{\boldsymbol{n}}$ satisfy the system (27). In order to derive an approximated solution in the low density limit, we introduce the variables $v_{\boldsymbol{n}}$ via the relation

$$h_{\boldsymbol{n}} = v_{\boldsymbol{n}}\rho. \tag{30}$$

When $\mathbf{n} = \mathbf{e}_\nu$, we use $v_{\boldsymbol{n}} = v_\nu$, so that the expression for the tracer velocity becomes

$$V = \frac{1}{\tau}(p_1 - p_{-1}) - \frac{\rho}{\tau}(p_1 - p_{-1} + p_1 v_1 - p_{-1} v_{-1}). \tag{31}$$

In the low density limit $\rho \to 0$ the coefficients A_μ can be approximated as

$$A_\mu \sim 1 + 2dx p_\mu, \qquad \alpha = \sum_\mu A_\mu \sim 2d(1+x), \tag{32}$$

and, substituting the expression (30) into (27), one obtains the system satisfied by the variables $v_{\boldsymbol{n}}$

$$2d(1+x)v_{\boldsymbol{n}} = \sum_{\nu=\pm1,2} [1 + 2dx p_\nu] v_{\boldsymbol{e}_\nu} \nabla_{-\nu}\mathcal{F}_{\boldsymbol{n}} - 2dx(p_1 - p_{-1})(\nabla_1 - \nabla_{-1})\mathcal{F}_{\boldsymbol{n}}, \tag{33}$$

where $x \equiv \tau^*/\tau$. Notice that the system (33) obtained in the low density approximation is linear in the variables $v_{\boldsymbol{n}}$.

A. Lorentz lattice gas limit

Let us consider the explicit case $d = 2$, in the limit of the standard Lorentz gas, namely when $x \to \infty$. Then the functions $\mathcal{F}_{\boldsymbol{n}}$ simplify to

$$\mathcal{F}_{\boldsymbol{n}} = e^{-n_1 F/2} \int_0^\infty e^{-t} \mathrm{I}_{n_1}(2t/Z)\mathrm{I}_{n_2}(2t/Z)dt, \tag{34}$$

with $Z = 2 + e^{\beta F/2} + e^{-\beta F/2}$. Introducing the variables u_i, with $i = \pm1, 2$, through the relation $v_i = (p_i - p_{-i})u_i$, we obtain the following linear system

$$\begin{aligned}
(p_1\nabla_{-1}\mathcal{F}_{\boldsymbol{e}_1} - 1)u_1 + (p_{-1}\nabla_1\mathcal{F}_{\boldsymbol{e}_1})u_{-1} + (2p_2\nabla_2\mathcal{F}_{\boldsymbol{e}_1})u_2 &= (\nabla_1 - \nabla_{-1})\mathcal{F}_{\boldsymbol{e}_1},\\
(p_1\nabla_{-1}\mathcal{F}_{\boldsymbol{e}_{-1}})u_1 + (p_{-1}\nabla_1\mathcal{F}_{\boldsymbol{e}_{-1}} - 1)u_{-1} + (2p_2\nabla_2\mathcal{F}_{\boldsymbol{e}_{-1}})u_2 &= (\nabla_1 - \nabla_{-1})\mathcal{F}_{\boldsymbol{e}_{-1}},\\
(p_1\nabla_{-1}\mathcal{F}_{\boldsymbol{e}_2})u_1 + (p_{-1}\nabla_1\mathcal{F}_{\boldsymbol{e}_2})u_{-1} + (p_2(\nabla_2 + \nabla_{-2})\mathcal{F}_{\boldsymbol{e}_2})u_2 &= (\nabla_1 - \nabla_{-1})\mathcal{F}_{\boldsymbol{e}_2}.
\end{aligned} \tag{35}$$

Notice that the expression (34) corresponds to the perturbed time evolution operator (integrated in time) introduced in Ref. [2]. In order to explicitly recover the solution reported in [2], we notice that, using the expressions for the probabilities $p_1 = e^{F/2}/Z$, $p_{-1} = e^{-F/2}/Z$ and $p_2 = 1/Z$, the following identities can be obtained

$$\begin{aligned}
\nabla_{-1}\mathcal{F}_{\boldsymbol{e}_1} &= \mathcal{F}_0 - e^{-F/2}\mathcal{F}_{\boldsymbol{e}_2} & \nabla_1\mathcal{F}_{\boldsymbol{e}_1} &= e^{-F}\mathcal{F}_{2\boldsymbol{e}_2} - e^{-F/2}\mathcal{F}_{\boldsymbol{e}_2}\\
\nabla_2\mathcal{F}_{\boldsymbol{e}_1} &= \mathcal{F}_{\boldsymbol{e}_1+\boldsymbol{e}_2} - e^{-F/2}\mathcal{F}_{\boldsymbol{e}_2} & (\nabla_1 - \nabla_{-1})\mathcal{F}_{\boldsymbol{e}_1} &= e^{-F}\mathcal{F}_{2\boldsymbol{e}_2} - \mathcal{F}_0\\
\nabla_{-1}\mathcal{F}_{\boldsymbol{e}_{-1}} &= e^{F}\mathcal{F}_{2\boldsymbol{e}_2} - e^{F/2}\mathcal{F}_{\boldsymbol{e}_2} & \nabla_1\mathcal{F}_{-\boldsymbol{e}_1} &= \mathcal{F}_0 - e^{F/2}\mathcal{F}_{\boldsymbol{e}_2}\\
\nabla_2\mathcal{F}_{\boldsymbol{e}_{-1}} &= e^{F}\mathcal{F}_{\boldsymbol{e}_1+\boldsymbol{e}_2} - e^{F/2}\mathcal{F}_{\boldsymbol{e}_2} & (\nabla_1 - \nabla_{-1})\mathcal{F}_{\boldsymbol{e}_{-1}} &= \mathcal{F}_0 - e^{F}\mathcal{F}_{2\boldsymbol{e}_2}\\
\nabla_1\mathcal{F}_{\boldsymbol{e}_2} &= \mathcal{F}_{\boldsymbol{e}_1+\boldsymbol{e}_2} - \mathcal{F}_{\boldsymbol{e}_2} & (\nabla_2 - \nabla_{-2})\mathcal{F}_{\boldsymbol{e}_2} &= \mathcal{F}_{2\boldsymbol{e}_2} + \mathcal{F}_0 - 2\mathcal{F}_{\boldsymbol{e}_2}\\
& & (\nabla_1 - \nabla_{-1})\mathcal{F}_{\boldsymbol{e}_2} &= (1 - e^{F})\mathcal{F}_{\boldsymbol{e}_1+\boldsymbol{e}_2}.
\end{aligned}$$

Finally, expressing the functions $\mathcal{F}_{\boldsymbol{e}_2}$ and $\mathcal{F}_{2\boldsymbol{e}_2}$ in terms of $\mathcal{F}_0$ and $\mathcal{F}_{\boldsymbol{e}_1+\boldsymbol{e}_2}$, namely

$$\mathcal{F}_{\boldsymbol{e}_2} = \frac{Z}{4}(\mathcal{F}_0 - 1), \qquad \mathcal{F}_{2\boldsymbol{e}_2} = \mathcal{F}_0\left(\frac{Z^2}{4} - 1\right) - 2e^{F/2}\mathcal{F}_{\boldsymbol{e}_1+\boldsymbol{e}_2} - \frac{Z^2}{4}, \tag{36}$$

one can check that from the system (35) the explicit solution reported in [2] follows.

B. Exact criterion for NDM in the low density limit

The solution of the system (33) gives the coefficients v_1 and v_{-1} appearing in the expression (31). These coefficients depend on x and on the probabilities $\{p_\nu\}$, $v_\mu = v_\mu(x, \{p_\nu\})$, both explicitly and implicitly through the functions $\mathcal{F}_{\boldsymbol{n}}$. In order to find the condition for negative differential mobility, we consider the case of large force, such that

$$p_1 = 1 - \epsilon \qquad p_{-1} = O(\epsilon^2) \qquad p_{\mu\neq\pm1} = \frac{\epsilon}{2d-2}, \tag{37}$$

where ϵ is a small quantity. Substituting these expressions into the definition of $\mathcal{F}_{\boldsymbol{n}}$, we can expand to the first order in ϵ to get

$$\mathcal{F}_{\boldsymbol{n}}(x,\epsilon) = \mathcal{F}^{(0)}_{\boldsymbol{n}}(x) + \epsilon\mathcal{F}^{(1)}_{\boldsymbol{n}}(x), \tag{38}$$

where $\mathcal{F}^{(0)}_{\boldsymbol{n}}(x) = \mathcal{F}_{\boldsymbol{n}}(x,\epsilon=0)$ and $\mathcal{F}^{(1)}_{\boldsymbol{n}}(x) = \frac{\partial}{\partial\epsilon}\mathcal{F}_{\boldsymbol{n}}(x,\epsilon)\big|_{\epsilon=0}$. Next, substituting Eqs. (37) and (38) into the solutions of the system (33), and retaining only the terms up to the order ϵ, we obtain the expression for the coefficients v_μ

$$v_\mu(x,\epsilon) = v^{(0)}_\mu(x) + \epsilon v^{(1)}_\mu(x). \tag{39}$$

Notice that $v^{(0)}_\mu(x)$ and $v^{(1)}_\mu(x)$ still have both an explicit and an implicit dependence on x, through the functions $\mathcal{F}^{(0)}_{\boldsymbol{n}}(x)$ and $\mathcal{F}^{(1)}_{\boldsymbol{n}}(x)$. Thus, for the tracer velocity (31) to the order ϵ we have

$$\begin{aligned}\tau V &= 1-\epsilon-\rho\left[1-\epsilon+(1-\epsilon)\left(v^{(0)}_1+\epsilon v^{(1)}_1\right)\right]\\ &= 1-\rho\left(1+v^{(0)}_1\right)-\epsilon\left[1-\rho\left(1+v^{(0)}_1-v^{(1)}_1\right)\right].\end{aligned} \tag{40}$$

Eventually, writing

$$V(x) = V^{(0)}(x) + \epsilon V^{(1)}(x), \tag{41}$$

with

$$V^{(0)}(x) = \frac{1}{\tau}\left[1-\rho\left(1+v^{(0)}_1(x)\right)\right] \tag{42}$$

$$V^{(1)}(x) = \frac{1}{\tau}\left[-1+\rho\left(1+v^{(0)}_1(x)-v^{(1)}_1(x)\right)\right], \tag{43}$$

a general criterion for negative differential mobility can be obtained by studying the sign of the term $V^{(1)}(x)$, which yields the condition

$$1-\rho H(x) < 0, \tag{44}$$

where

$$H(x) = 1+\left[v^{(0)}_1(x)-v^{(1)}_1(x)\right]. \tag{45}$$

The functions $v^{(0)}_1(x)$ and $v^{(1)}_1(x)$ satisfy the system obtained by expanding (33) to the first order in ϵ. In particular, in the case $d=2$, to the zero order we have

$$A_0 V_0 = B_0, \tag{46}$$

where, dropping the dependence on x in the functions $\mathcal{F}_{\boldsymbol{n}}$,

$$A_0 = \begin{pmatrix} \mathcal{F}^{(0)}_{0,0}+4x(\mathcal{F}^{(0)}_{0,0}-\mathcal{F}^{(0)}_{1,0}-1)-\mathcal{F}^{(0)}_{1,0}-4 & \mathcal{F}^{(0)}_{2,0}-\mathcal{F}^{(0)}_{1,0} & 2\mathcal{F}^{(0)}_{1,1}-2\mathcal{F}^{(0)}_{1,0} \\ (4x+1)(\mathcal{F}^{(0)}_{-2,0}-\mathcal{F}^{(0)}_{-1,0}) & -4x-\mathcal{F}^{(0)}_{-1,0}+\mathcal{F}^{(0)}_{0,0}-4 & 2\mathcal{F}^{(0)}_{-1,1}-2\mathcal{F}^{(0)}_{-1,0} \\ (4x+1)(\mathcal{F}^{(0)}_{-1,1}-\mathcal{F}^{(0)}_{0,1}) & \mathcal{F}^{(0)}_{1,2}-\mathcal{F}^{(0)}_{0,2} & -4x+\mathcal{F}^{(0)}_{0,0}-2\mathcal{F}^{(0)}_{0,1}+\mathcal{F}^{(0)}_{0,2}-4 \end{pmatrix}, \tag{47}$$

$$V_0 = \begin{pmatrix} v^{(0)}_1 \\ v^{(0)}_{-1} \\ v^{(0)}_2 \end{pmatrix}, \tag{48}$$

and

$$B_0 = \begin{pmatrix} 4x(\mathcal{F}^{(0)}_{2,0} - \mathcal{F}^{(0)}_{0,0}) \\ 4x(\mathcal{F}^{(0)}_{0,0} - \mathcal{F}^{(0)}_{-2,0}) \\ 4x(\mathcal{F}^{(0)}_{1,1} - \mathcal{F}^{(0)}_{-1,1}) \end{pmatrix}. \tag{49}$$

Therefore

$$v^{(0)}_1 = \frac{\det \tilde{A}_0}{\det A_0}, \tag{50}$$

where $\tilde{A}_0$ is obtained from A_0 replacing the first column with the vector B_0. Analogously, for $v^{(1)}_1$, we have to solve the system

$$A_1 V_1 = B_1, \tag{51}$$

where

$$A_1 = \begin{pmatrix} \mathcal{F}^{(0)}_{0,0} + 4x(\mathcal{F}^{(0)}_{0,0} - \mathcal{F}^{(0)}_{1,0} - 1) - \mathcal{F}^{(0)}_{1,0} - 4 & \mathcal{F}^{(0)}_{2,0} - \mathcal{F}^{(0)}_{1,0} & 2\mathcal{F}^{(0)}_{1,1} - 2\mathcal{F}^{(0)}_{1,0} \\ (4x+1)(\mathcal{F}^{(0)}_{-2,0} - \mathcal{F}^{(0)}_{-1,0}) & -4x - \mathcal{F}^{(0)}_{-1,0} + \mathcal{F}^{(0)}_{0,0} - 4 & 2\mathcal{F}^{(0)}_{-1,1} - 2\mathcal{F}^{(0)}_{-1,0} \\ (4x+1)(\mathcal{F}^{(0)}_{-1,1} - \mathcal{F}^{(0)}_{0,1}) & \mathcal{F}^{(0)}_{1,2} - \mathcal{F}^{(0)}_{0,2} & -4x + \mathcal{F}^{(0)}_{0,0} - 2\mathcal{F}^{(0)}_{0,1} + \mathcal{F}^{(0)}_{0,2} - 4 \end{pmatrix}, \tag{52}$$

$$V_1 = \begin{pmatrix} v^{(1)}_1 \\ v^{(1)}_{-1} \\ v^{(1)}_2 \end{pmatrix}, \tag{53}$$

and

$$B_1 = \begin{pmatrix} B_{11} \\ B_{12} \\ B_{13} \end{pmatrix}, \tag{54}$$

with

$$\begin{aligned} B_{11} &= -v^{(0)}_1(\mathcal{F}^{(1)}_{0,0} - \mathcal{F}^{(1)}_{1,0}) + 2v^{(0)}_2\mathcal{F}^{(1)}_{1,0} + v^{(0)}_{-1}\mathcal{F}^{(1)}_{1,0} - 2v^{(0)}_2\mathcal{F}^{(1)}_{1,1} - v^{(0)}_{-1}\mathcal{F}^{(1)}_{2,0} \\ &\quad + 4x\left[(v^{(0)}_1 + 1)\mathcal{F}^{(0)}_{0,0} + v^{(0)}_2\mathcal{F}^{(0)}_{1,0} - v^{(0)}_2\mathcal{F}^{(0)}_{1,1} - \mathcal{F}^{(0)}_{2,0} - \mathcal{F}^{(1)}_{0,0} - v^{(0)}_1(\mathcal{F}^{(0)}_{1,0} + \mathcal{F}^{(1)}_{0,0} - \mathcal{F}^{(1)}_{1,0}) + \mathcal{F}^{(1)}_{2,0}\right], \end{aligned} \tag{55}$$

$$\begin{aligned} B_{12} &= -v^{(0)}_1(\mathcal{F}^{(1)}_{-2,0} - \mathcal{F}^{(1)}_{-1,0}) + 2v^{(0)}_2\mathcal{F}^{(1)}_{-1,0} + v^{(0)}_{-1}\mathcal{F}^{(1)}_{-1,0} - 2v^{(0)}_2\mathcal{F}^{(1)}_{-1,1} - v^{(0)}_{-1}\mathcal{F}^{(1)}_{0,0} \\ &\quad + 4x\left[(v^{(0)}_1 + 1)\mathcal{F}^{(0)}_{-2,0} + v^{(0)}_2\mathcal{F}^{(0)}_{-1,0} - v^{(0)}_2\mathcal{F}^{(0)}_{-1,1} - \mathcal{F}^{(0)}_{0,0} - \mathcal{F}^{(1)}_{-2,0} - v^{(0)}_1(\mathcal{F}^{(0)}_{-1,0} + \mathcal{F}^{(1)}_{-2,0} - \mathcal{F}^{(1)}_{-1,0}) + \mathcal{F}^{(1)}_{0,0}\right], \end{aligned} \tag{56}$$

$$\begin{aligned} B_{13} &= -v^{(0)}_2\mathcal{F}^{(1)}_{0,0} - v^{(0)}_1(\mathcal{F}^{(1)}_{-1,1} - \mathcal{F}^{(1)}_{0,1}) + 2v^{(0)}_2\mathcal{F}^{(1)}_{0,1} - v^{(0)}_2\mathcal{F}^{(1)}_{0,2} + v^{(0)}_{-1}\mathcal{F}^{(1)}_{0,2} \\ &\quad - 2x\big[-2(v^{(0)}_1 + 1)\mathcal{F}^{(0)}_{-1,1} + v^{(0)}_2(\mathcal{F}^{(0)}_{0,0} - 2\mathcal{F}^{(0)}_{0,1} + \mathcal{F}^{(0)}_{0,2}) \\ &\quad + 2(\mathcal{F}^{(0)}_{1,1} + \mathcal{F}^{(1)}_{-1,1} + v^{(0)}_1(\mathcal{F}^{(0)}_{0,1} + \mathcal{F}^{(1)}_{-1,1} - \mathcal{F}^{(1)}_{0,1}) - \mathcal{F}^{(1)}_{1,1})\big] - v^{(0)}_{-1}\mathcal{F}^{(1)}_{1,2}. \end{aligned} \tag{57}$$

Therefore

$$v^{(1)}_1 = \frac{\det \tilde{A}_1}{\det A_1}, \tag{58}$$

where $\tilde{A}_1$ is obtained from A_1 replacing the first column with the vector B_1.

In order to obtain an explicit formula for $v^{(0)}_1(x)$ and $v^{(1)}_1(x)$ we expand the complete solutions in $1/x$. This provides the leading contribution of the function $H(x)$ for $x \to \infty$, which corresponds to the large τ^*/τ limit. First, we write the expressions for $\mathcal{F}^{(0)}_{\boldsymbol{n}}(x)$ and $\mathcal{F}^{(1)}_{\boldsymbol{n}}(x)$:

$$\mathcal{F}^{(0)}_{\boldsymbol{n}}(x) = (1+4x)^{-n_1/2}\int_0^\infty dt\ e^{-t}\mathrm{I}_{n_1}[t\sqrt{1+4x}/(2+2x)]\mathrm{I}_{n_2}[t/(2+2x)], \tag{59}$$

$$\begin{aligned} \mathcal{F}^{(1)}_{\boldsymbol{n}}(x) &= x\epsilon(4x+1)^{-n_1/2}\int_0^\infty dt\ e^{-t} \\ &\quad \times \left[\mathrm{I}_{n_1}\left(\frac{t\sqrt{4x+1}}{2x+2}\right)\left(2n_2\mathrm{I}_{n_2}\left(\frac{t}{2x+2}\right) + \frac{t\mathrm{I}_{n_2+1}\left(\frac{t}{2x+2}\right)}{x+1}\right) - \frac{t\mathrm{I}_{n_1+1}\left(\frac{t\sqrt{4x+1}}{2x+2}\right)\mathrm{I}_{n_2}\left(\frac{t}{2x+2}\right)}{(x+1)\sqrt{4x+1}}\right]. \end{aligned} \tag{60}$$

Then, developing in $1/x$ these expressions up to the order $1/x^2$, we get

$$\mathcal{F}_{\boldsymbol{n}}^{(0)}(x) = \int_0^\infty dt\ e^{-t}\left[G_{\boldsymbol{n}}^{(0,0)}(t) + \frac{1}{x}G_{\boldsymbol{n}}^{(0,1)}(t) + \frac{1}{x^2}G_{\boldsymbol{n}}^{(0,2)}(t) + O\left(\frac{1}{x^3}\right)\right], \tag{61}$$

and

$$\mathcal{F}_{\boldsymbol{n}}^{(1)}(x) = \int_0^\infty dt\ e^{-t}\left[G_{\boldsymbol{n}}^{(1,0)}(t) + \frac{1}{x}G_{\boldsymbol{n}}^{(1,1)}(t) + \frac{1}{x^2}G_{\boldsymbol{n}}^{(1,2)}(t) + O\left(\frac{1}{x^3}\right)\right]. \tag{62}$$

Using the expansions (61) and (62) in the solutions for $v_1^{(0)}$ and $v_1^{(1)}$ we get

$$v_1^{(0)}(x) = 2x - \frac{7}{4x} + \frac{69}{64x^2} + o\left(\frac{1}{x}\right)^3, \tag{63}$$

$$v_1^{(1)}(x) = -4x^2 - x + 8 - \frac{1}{8x} - \frac{553}{64x^2} + o\left(\frac{1}{x}\right)^3. \tag{64}$$

$$\tag{65}$$

Finally, using Eq. (45), we obtain

$$H(x) = -7 + \frac{311}{32x^2} - \frac{13}{8x} + 3x + 4x^2 \underset{x\to\infty}{\sim} 4x^2, \tag{66}$$

and, thus, the condition on the density ρ, Eq. (44), yields

$$\rho \underset{x\to\infty}{\sim} \frac{1}{4x^2}. \tag{67}$$

III. EXPLICIT SOLUTION FOR HIGH DENSITY

Introducing the vacancy density $\rho_0 \equiv 1-\rho$, and considering the case $d=2$, for the coefficients A_ν one has

$$A_\nu = 1 + \frac{4\tau^*}{\tau}p_\nu(\rho_0 - h_\nu), \tag{68}$$

and

$$A_1 - A_{-1} = \frac{4\tau^*}{\tau}[\rho_0(p_1 - p_{-1}) - p_1 h_1 + p_{-1}h_{-1}]. \tag{69}$$

In the high density limit, $\rho_0 \to 0$, the system satisfied by the functions h_ν

$$\begin{aligned}\alpha(h_1 - h_{-1}) = &\sum_\nu A_\nu h_\nu \nabla_{-\nu}(\mathcal{F}_{1,0} - \mathcal{F}_{-1,0}) \\ &- (1-\rho_0)(A_1 - A_{-1})(\nabla_1 - \nabla_{-1})(\mathcal{F}_{1,0} - \mathcal{F}_{-1,0}),\end{aligned} \tag{70}$$

can be linearized, yielding the solutions

$$h_{\pm 1} = \mp \frac{\rho_0 \frac{4\tau^*}{\tau}(p_1 - p_{-1})(\mathcal{F}_{2,0} - \mathcal{F}_{0,0})}{4 + (\mathcal{F}_{0,0} - \mathcal{F}_{0,2})\left[\frac{4\tau^*}{\tau}(p_1 + p_{-1}) - 1\right]}. \tag{71}$$

Substituting Eq. (71) into (69), and using the definition $A_\nu \equiv 1 + \frac{2d\tau^*}{\tau}p_\nu(1 - k(\boldsymbol{e}_\nu))$, one obtains the tracer velocity

$$V(\rho \to 1) = \frac{1}{\tau}(p_1 - p_{-1})\rho_0 \frac{1}{1 + \frac{4\tau^*}{\tau}\frac{(p_1 + p_{-1})(4 - 8/\pi)}{8/\pi}}, \tag{72}$$

where we have used the result $\mathcal{F}_{0,0} - \mathcal{F}_{2,0} = 4 - \frac{8}{\pi}$ [1]. Let us notice that Eq. (72) is valid for a general choice of p_ν. In particular, using the definition of the probabilities in Eq. (1) of the main text, one immediately recovers the final result reported in Eq. (13) of the letter.

IV. NUMERICAL SIMULATIONS

We consider a $d-$dimensional lattice with M sites and prepare the N particles in a random configuration, with density $\rho = N/M$. In the case $d = 2$ for $\rho \leq 0.2$, we used a square lattice with $M = L_x \times L_y = 100^2$ sites, with periodic boundary conditions in both directions, and we checked that results are independent of the box size. In the case $\rho = 0.5$, to avoid finite size effects, we used $L_x = L_y = 250$. For $d = 3$, the box linear size is $L = 60$, with periodic boundary conditions. In Fig 3 we compare analytic and numerical results for the case $d = 3$.

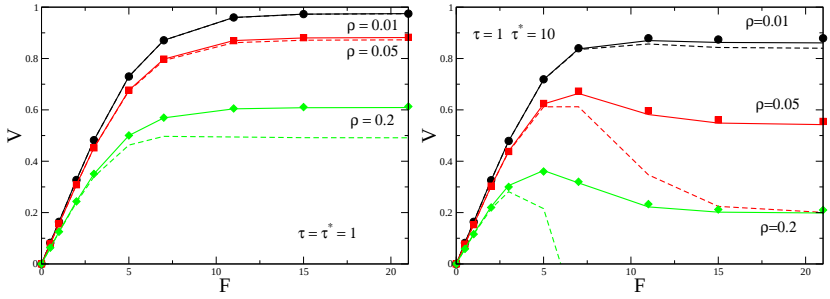

FIG. 3. 3D lattice: Analytic prediction (continuous lines), numerical simulations (points) and explicit solution in the low density approximation (dashed lines) for the force velocity relation $V(F)$ in the case $d = 3$, with $\tau = \tau^* = 1$ (left panel) and $\tau = 1$, $\tau^* = 10$ (right panel).

[1] B. D. Hughes, *Random Walks and Random Environments* (Oxford Science, Oxford, 1995).
[2] S. Leitmann and T. Franosch, Phys. Rev. Lett. **111**, 190603 (2013).